DETERMINING TARGETS FOR PERSONALIZED MULTITARGET NONINVASIVE STIMULATION OF THE FRONTOPARIETAL CONTROL NETWORK

Poydasheva AG ✉, Sinitsyn DO, Bakulin IS, Zabirova AH, Lagoda DYu, Suponeva NA, Piradov MA

Russian Center of Neurology and Neurosciences, Moscow, Russia

Personalization of selecting a target for rTMS is a problem, solving which can significantly increase the method efficacy. Stimulation of the key hubs of individual-level resting-state networks represents an approach to personalization. The study aimed to develop an rTMS personalization method based on the selection of individual frontoparietal control network (FPCN) hubs and assessment of their localization variability. To determine the FPCN hubs, individual maps were built using the FPCN group mask as a seed. The searchlight algorithm with the sphere radius of 5 mm was used to select targets within the dorsolateral prefrontal cortex (DLPFC) and posterior parietal cortex (PPC). The target spatial localization variability and correctness of using the routine "5 cm rule" for the DLPFC localization were analyzed. In 24 healthy volunteers (9 males, average age 29±7 years), high interindividual variability of targets was demonstrated. In no area is there a universal position of the stimulation coil that would effectively stimulate targets in all volunteers. Spatial dispersion of points is higher in the DLPFC (volumes of the polyhedra containing the point sets are 2095 mm^3 in the DLPFC and 739 mm^3 in the PPC). All individual targets in the DLPFC are located within the FPCN mask, while in the PPC some targets are outside this mask. The average distance between the M1 zones and DLPFC is 64±13 mm. In 75% of the subjects, this exceeds 5 cm, which confirms that it was incorrect to use the routine "5 cm rule" for coil positioning in the majority of subjects. An algorithm to select personalized targets for rTMS based on the resting-state fMRI data in the DLPFC and PPC being the key FPCN hubs has been developed.

Keywords: multitarget transcranial magnetic stimulation, personalization, resting-state networks, frontoparietal control network

Funding: the study was conducted as part of the project "Developing a Transcranial Magnetic Stimulation Method to Improve Cognitive Functions in Healthy Individuals" implemented within the framework of the National Project "New Health Preservation Technologies" (registration number 1025020400006-8-3.2.25).

Author contribution: Poydasheva AG, Sinitsyn DO, Bakulin IS — study planning and design; Poydasheva AG, Zabirova AH — literature review; Bakulin IS, Zabirova AH, Lagoda DYu — data acquisition; Sinitsyn DO, Poydasheva AG — data analysis; Poydasheva AG, Sinitsyn DO — manuscript writing; all authors — data interpretation, manuscript editing.

Compliance with ethical standards: the study was approved by the Ethics Committee of the Russian Center of Neurology and Neurosciences (protocol No. 5-1/25 dated 19 May 2025). All the volunteers signed the informed consent form.

✉ **Correspondence should be addressed:** Alexandra G. Poydasheva
Volokolamskoye shosse, 80, Moscow, 125310, Russia; poydasheva@neurology.ru

Received: 14.11.2025 **Accepted:** 10.12.2025 **Published online:** 20.12.2025

DOI: 10.24075/brsmu.2025.081

ОПРЕДЕЛЕНИЕ МИШЕНЕЙ ДЛЯ ПЕРСОНАЛИЗИРОВАННОЙ МУЛЬТИТАРГЕТНОЙ НЕИНВАЗИВНОЙ СТИМУЛЯЦИИ ЛОБНО-ТЕМЕННОЙ СЕТИ КОНТРОЛЯ

А. Г. Пойдашева ✉, Д. О. Синицын, И. С. Бакулин, А. Х. Забирова, Д. Ю. Лагода, Н. А. Супонева, М. А. Пирадов

Российский центр неврологии и нейронаук, Москва, Россия

Персонализация выбора мишени для рТМС — актуальная задача, решение которой может значительно увеличить эффективность метода. Один из подходов к персонализации — стимуляция ключевых хабов индивидуальных сетей покоя. Цель исследования — разработка методологии персонализации рТМС на основе выделения индивидуальных хабов фронто-париетальной контрольной сети (FPCN) с оценкой вариабельности их локализации. Для определения хабов FPCN были построены индивидуальные карты с использованием в качестве seed групповой маски сети FPCN. С помощью алгоритма прожектора с радиусом сферы 5 мм были выбраны мишени в пределах дорсолатеральной префронтальной коры (ДЛПФК) и задней теменной коры (ЗТК). Анализировали вариабельность пространственной локализации мишеней и корректность применения рутинного «правила 5 см» для локализации ДЛПФК. У 24 здоровых добровольцев (9 мужчин, средний возраст 29±7 лет) продемонстрирована высокая межиндивидуальная вариабельность мишеней. Ни в одной из областей не существует универсального положения стимулирующей катушки, позволившего бы эффективно стимулировать мишени у всех добровольцев. Пространственный разброс точек выше в ДЛПФК (объемы многогранников, содержащих множества точек равны 2095 $мм^3$ в ДЛПФК и 739 $мм^3$ в ЗТК). Все индивидуальные мишени в ДЛПФК лежат в пределах маски FPCN, а для ЗТК ряд мишеней находится вне этой маски. Среднее расстояние между зоной кисти первичной моторной коры (М1) и ДЛПКК составило 64±13 мм. У 75% участников это расстояние превышало 5 см, что подтверждает некорректность применения рутинного «правила 5 см» позиционирования катушки для большинства испытуемых. Разработан алгоритм выбора персонализированных мишеней для рТМС по данным фМРТ покоя в ДЛПФК и ЗТК, которые являются ключевыми хабами FPCN.

Ключевые слова: мультитаргетная транскраниальная магнитная стимуляция, персонализация, сети покоя, лобно-теменная сеть контроля

Финансирование: исследование выполнено в рамках проекта «Разработка методики транскраниальной магнитной стимуляции для улучшения когнитивных функций у здоровых лиц», выполняемого в ходе Национального проекта «Новые технологии сбережения здоровья» (рег. №1025020400006-8-3.2.25).

Вклад авторов: А. Г. Пойдашева, Д. О. Синицын, И. С. Бакулин — планирование и дизайн исследования; А. Г. Пойдашева, А. Х. Забирова — анализ литературы; И. С. Бакулин, А. Х. Забирова, Д. Ю. Лагода — сбор данных; Д. О. Синицын, А. Г. Пойдашева — анализ данных; А. Г. Пойдашева, Д. О. Синицын — подготовка статьи; все авторы — интерпретация данных, редактирование статьи.

Соблюдение этических стандартов: исследование одобрено этическим комитетом ФГБНУ РЦНН (протокол № 5-1/25 от 19 мая 2025 г.). Все добровольцы подписали форму добровольного информированного согласия.

✉ **Для корреспонденции:** Александра Георгиевна Пойдашева
Волоколамское шоссе, д. 80, г. Москва, 125367, Россия; poydasheva@neurology.ru

Статья получена: 14.11.2025 **Статья принята к печати:** 10.12.2025 **Опубликована онлайн:** 20.12.2025

DOI: 10.24075/vrgmu.2025.081

Repetitive transcranial magnetic stimulation (rTMS) is a noninvasive neuromodulation method widely used in research and clinical practice [1]. The rTMS protocols have long-term effects similar to the synaptic plasticity mechanisms: high-frequency protocols and intermittent theta-burst stimulation have an effect similar to the long-term potentiation (LTP-like), increasing the stimulated cortex area excitability, while low-frequency protocols and continuous theta-burst stimulation have an effect similar to the long-term depression (LTD-like), decreasing the stimulated area excitability [2]. In recent years, the rTMS neural network effects represented by the possibility of modulating activity of not only the stimulated zone, but also distant brain areas structurally or functionally connected to this zone, are extensively discussed [3, 4].

The high effect variability, one of the possible reasons for which is considered to be suboptimal selection of a target for stimulation, is an important issue of using rTMS in both clinical and research practice. The size of most stimulated anatomical regions is larger than the size of the focus of the magnetic field generated by the stimulation coil, which results in a large number of possible variants of coil positioning within the region. Furthermore, various zones located within these anatomical regions can have different cytoarchitecture, as well as structural and functional connectivity, which is especially important in the context of the rTMS neural network effects [5, 6].

The emergence of TMS neuronavigation systems and algorithms to calculate the TMS-induced electric field maximum made it possible to control the stimulation coil position relative to individual structural data of the patient's MRI in real time, as well as to considerably increase the coil positioning accuracy [7]. Moreover, neuronavigation systems allowed one to use functional MRI data (both group and individual) for targeting, thereby opening up new opportunities for the personalized identification and influence on the selected targets [8]. Various approaches to personalized target identification based on functional MRI in the resting state and with different paradigms are being explored. The personalized determination of the localization of "hubs" of a particular resting-state network represents one such approach. In this case the main hypothesis is that there is a possibility of providing the TMS neural network effects and modulating the activity of a certain network when stimulating one or more network "hubs".

There are a number of methodological issues related to both individual allocation of the resting-state networks and determination of the target itself based on the activation maps identified. For example, several algorithms for allocation of individual resting-state networks were proposed: iterative (see [9] for details), Infomap algorithm [10], multi-session hierarchical Bayesian model (MS-HBM) [11], independent component analysis (ICA), etc. A point, the signal of which reaches the maximum of the functional connectivity characteristic of interest, can be specified as a target within the selected connectivity map [12], or a number of approaches can be used considering connectivity of the zones surrounding this point. For example, the searchlight algorithm selects the point with the maximum average value of the functional connectivity characteristic of interest over the sphere with the specified radius having the center in this point [13], while the cluster algorithm uses the specified threshold to cut off the cluster with the maximum signal and use the coordinates of the center of mass of this cluster [14].

The fronto-parietal control network (FPCN) is one of the networks most consistently identified in resting-state fMRI, the activity of which is associated with cognitive activity [15, 16]. The major FPCN hubs located superficially and accessible for rTMS are the dorsolateral prefrontal cortex (DLPFC) and posterior parietal cortex (PPC). The studies have shown the possibility of modulating cognitive functions in the population of healthy subjects and patients when conducting rTMS of these regions without using a personalized approach, however, the results of these studies are heterogeneous due to high effect variability [17–19].

The objective of this study was to develop a method for personalized identification of the targets for transcranial magnetic stimulation based on the identification of individual FPCN hubs within the DLPFC and PPC with assessment of variability of localization of such targets in healthy volunteers.

METHODS

The study was conducted at the Russian Center of Neurology and Neurosciences in 2025. Medical history and demographic data were collected for all healthy volunteers.

Subjects

Inclusion criteria: the informed consent availability; age 20–50 years. Exclusion criteria: refusal to participate in the study; contraindications for MRI; a neurological disorder affecting cognitive functions or a mental disorder at the time of enrollment or a history of such disorders; a chronic severe somatic disorder, decompensated chronic disorder or acute phase of the disease (for example, ARVI).

A total of 24 healthy volunteers aged 21–48 years (9 males, average age 29 years, standard deviation 7 years) were included in the study.

All volunteers underwent neuroimaging assessment on a 3 T Siemens MAGNETOM Prisma scanner (Germany).

MRI data acquisition and pre-processing

The neuroimaging assessment protocol included the T1-weighted imaging mode with the Multi-Planar Reconstruction (MPR) option for structural data acquisition (TR 2300 ms, voxel 1 × 1 × 1 mm^3) and the Multiplanar Gradient Echo mode (TR 1500 ms, voxel 2 × 2 × 2.2 mm^3) to record the resting-state fMRI signal for analysis of functional connectivity.

The MRI data were analyzed using the CONN (Functional Connectivity SPM Toolbox 2017, McGovern Institute for Brain Research, Massachusetts Institute of Technology (http://www.nitrc.org/projects/conn), Cambridge, USA) version 22.v2407, and SPM12 (Functional Imaging Laboratory, Wellcome Department of Imaging Neuroscience, Institute of Neurology (http://www.fil.ion.ucl.ac.uk/spm/software), London, UK) software packages. Functional images were subjected to realignment with susceptibility distortion correction using field maps, slice timing correction, outlier identification. The structural data were segmented into tissues and normalized into the MNI (Montreal Neurological Institute) space, while functional data were normalized using the deformation field calculated for structural data (indirect normalization). Spatial smoothing was applied to functional data with a Gaussian filter with the full width at half maximum (FWHM) kernel size of 8 mm. Furthermore, the average signal for the region, the connectivity with which was calculated (in the seed-to-voxel procedure described below), was determined based on the unsmoothed data in order to avoid mixing with the signal from adjacent regions.

Furthermore, regression was used to delete contributions of artifacts proportional to the signal of white matter (five principal

Table. Individual coordinates of targets in the left dorsolateral prefrontal cortex and posterior parietal cortex

No	Cortical area						Distance between M1 and the target in the DLPFC, mm
	DLPFC			PPC			
	X-axis coordinate	*Y*-axis coordinate	*Z*-axis coordinate	*X*-axis coordinate	*Y*-axis coordinate	*Z*-axis coordinate	
1	–41	51	14	–27	–69	59	75
2	–45	48	6	–46	–57	52	76
3	–47	28	36	–39	–60	57	44
4	–41	47	21	–46	–48	58	68
5	–41	34	36	–54	–40	52	50
6	–43	48	14	–51	–53	50	72
7	–44	47	14	–51	–48	52	71
8	–49	28	32	–51	–47	52	46
9	–43	47	13	–55	–42	51	72
10	–51	21	34	–38	–72	46	39
11	–50	25	30	–39	–64	54	44
12	–46	46	9	–50	–52	52	72
13	–44	39	28	–56	–42	50	57
14	–47	43	8	–50	–51	53	71
15	–45	24	42	–45	–61	51	39
16	–42	52	6	–52	–48	51	80
17	–48	43	9	–51	–51	51	70
18	–41	40	30	–46	–57	54	59
19	–45	46	11	–60	–29	44	72
20	–40	35	37	–58	–42	46	51
21	–44	47	12	–57	–49	43	72
22	–40	51	17	–43	–54	57	73
23	–46	47	6	–46	–49	58	75
24	–45	48	6	–45	–54	56	76

Note: DLPFC — dorsolateral prefrontal cortex, PPC — posterior parietal cortex, M1 — primary motor cortex.

components), cerebrospinal fluid (five principal components), motion parameters and their first order derivatives (12 regressors), outlier scans, session effect and its first-order derivative (two regressors), as well as the linear trend (two regressors) from functional data, with subsequent band-pass filtering in the 0.008–0.09 Hz range.

Resting-state fMRI data analysis aimed at selecting targets for stimulation

The literature dedicated to solving the problem of finding an invidual parcellation of the cortical surface into functional resting-state networks and selecting an optimal point in the zones available within this network fragment was reviewed. An optimal set of approaches was identified at each stage of data analysis, which was later combined into an algorithm for selecting personalized targets for rTMS. The main steps of this algorithm are provided below.

Algorithm to select personalized targets for rTMS belonging to the fronto-parietal control network (FPCN)

Step 1. Construction of the map of the degree to which points in the brain belong to the FPCN.

The seed-to-voxel method is used: calculation of connectivity of the given region (referred to as seed region) with other voxels of the brain. The method is applied to individual resting-state fMRI data. The FPCN mask generated in the study [20] based on the average connectivity of the group of 1000 healthy volunteers is used as the seed region. The resulting seed connectivity map is used as a map of the degree to which points in the brain belong to the FPCN.

Step 2. Creating a set of candidate voxels for selection of targets located on the brain surface.

Voxels located on the brain surface are selected. For that the function spm_erode is applied to the intracranial volume mask from the SPM package transformed into the specific subject's individual space. This function calculates the region obtained from the specified region by removing one layer of voxels from its surface. Voxels removed by this function are calculated by subtraction of intracranial volume masks before and after the spm_erode application. The set of these voxels is taken as the intracranial volume margin; targets are further selected among these voxels.

Step 3. Selection of the candidate voxels located within the specified target regions.

The ones located within the target regions, DLPFC and PPC, are selected among the voxels obtained in the previous step. The left DLPFC was defined as the portion of the left middle frontal gyrus, excluding the premotor cortex. The mask of the left middle frontal gyrus was taken from the atlas created by A. Hammers and colleagues [21]. The mask of the premotor

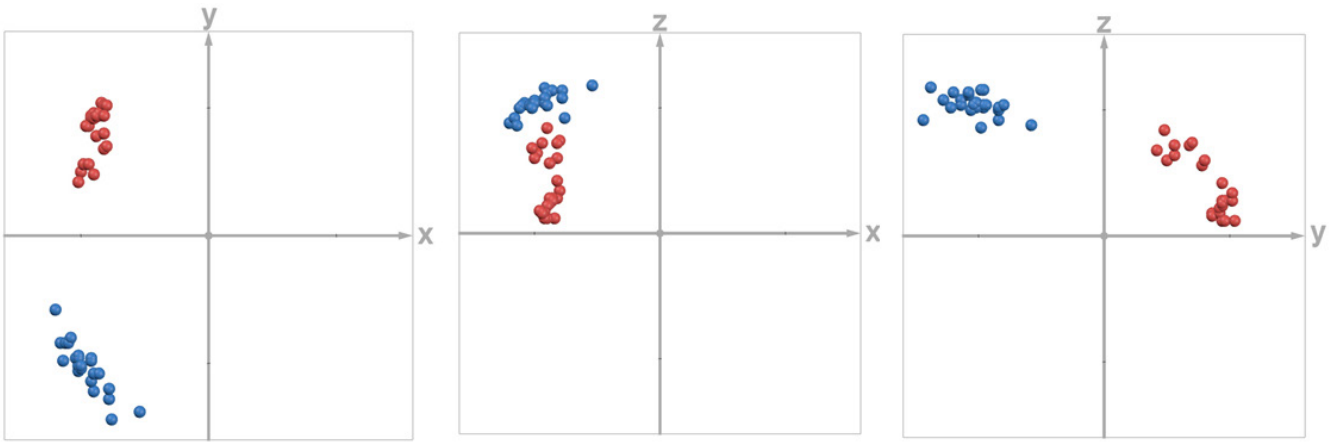

Fig. 1. Projections of targets in 24 subjects on coordinate planes. Red are targets in the DLPFC, blue are targets in the posterior parietal cortex

cortex was obtained by merging areas of the left dorsal and ventral premotor cortex from the HMAT (Human Motor Area Template, [22]). The left posterior parietal cortex was defined as the union of the left supramarginal and angular gyri and the superior parietal lobule from the atlas by A. Hammers.

Step 4. Selection of targets by the searchlight method [13, 14].

The quality measure equal to the mean of the values of the above seed connectivity map within the sphere with the center in a given voxel and the 5 mm radius is calculated for each voxel selected in the previous steps (to consider the effect of stimulation on a certain cortical region surrounding the target point). Voxels with the maximum quality measure values within each target region are selected as targets.

Analysis of the target spatial localization

Individual targets for each subject were transformed into the MNI space using the deformation field transforming the structural image into this space that was generated during MRI data pre-processing. Group mean values and standard deviations of the coordinates of these targets were calculated to describe the distribution of their localization in different subjects. Distances between the targets in the DLPFC and the motor cortex in the hand muscle cortical representation area were calculated. For that the group map of activation (for 486 subjects) upon moving the right fingers based on the Human Connectome Project data [21] was used, downloaded from the Neurovault database (dataset ID https://identifiers.org/neurovault.image:3162). This map was binarized with the threshold Z > 22 selected in such a way as to highlight the cluster in the precentral gyrus region, without including other nearby clusters. The distance to the closest voxel in the resulting binarized activation map was calculated for each target in the DLPFC.

RESULTS

An algorithm for determining the coordinates of points within individual FPCN hubs in the DLPFC and PPC that could be used as targets for rTMS was developed based on the literature review.

Coordinates of targets in two cortical regions were determined for each volunteer (Table).

After transforming each target to the MNI space the group-mean coordinates of targets in the DLPFC are –44.6, 41.1, 19.7 mm, standard deviations are 3.1, 9.5, 12.0 mm. The mean coordinates of targets in the PPC are –48.2, –51.7, 52.0 mm, standard deviations are 7.6, 9.6, 4.2 mm. For the DLPFC, the mean distance between the target and its midpoint is 14.3 mm, the maximum distance is 28.3 mm, for PPC these are 10.4 mm and 28 mm, respectively. The maximum distance

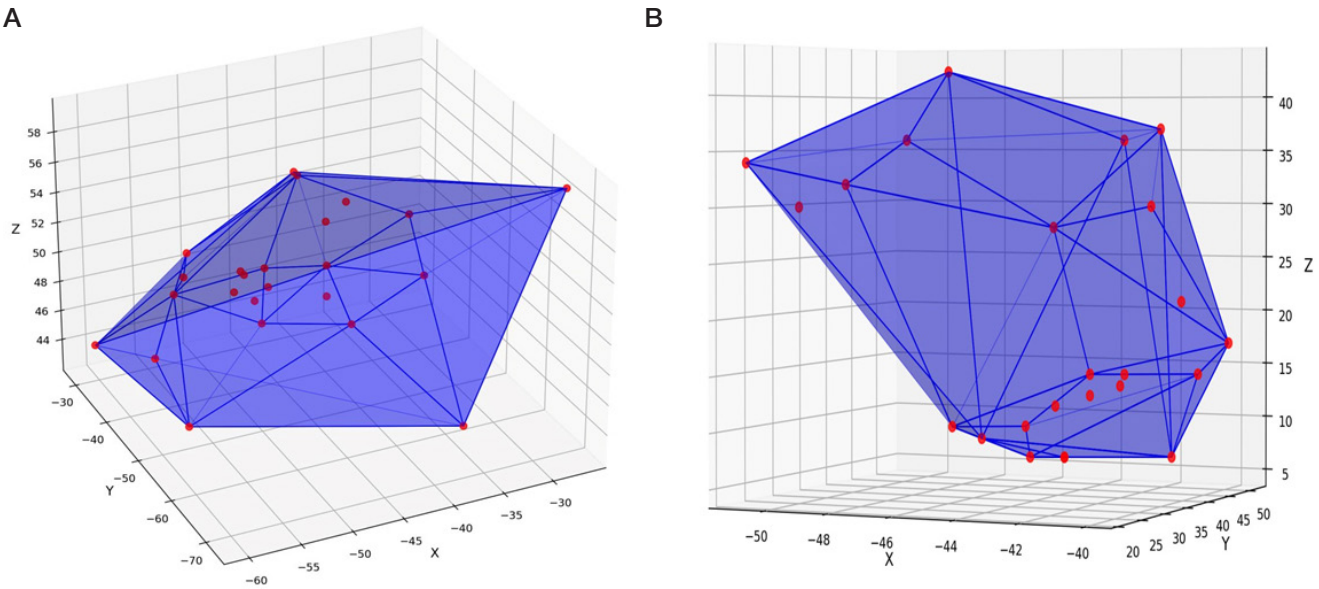

Fig. 2. Convex hulls of sets of points with the coordinates of targets in the PPC (Fig. A) and DLPFC (Fig. B)

between pairs of targets is 45.9 mm in the DLPFC, 54.1 mm in the PPC (Fig. 1).

Despite comparable linear measures of target dispersion, the volumes of polyhedra calculated by the convex hull method and containing sets of points for each of the assessed regions reported for the DLPFC turned out to be almost 3 times higher than that reported for the PPC (2095 and 739 mm^3, respectively) (Fig. 2).

When superimposing targets on the FPCN mask used as a seed region for individual connectivity calculations, in the DLPFC all targets were within the mask, while in the PPC some targets were beyond the mask (Fig. 3).

When estimating distances from individual targets in the DLPFC to the primary motor cortex (M1), the mean value was 64 mm, standard deviation was 13 mm (Table 1). Furthermore, only 6 volunteers had distances (25%) not exceeding 50 mm.

DISCUSSION

In the study, we proposed a personalized target selection algorithm based on selection of individual FPCN hubs within the DLPFC and PPC. High interindividual variability of targets was demonstrated. Furthermore, spatial dispersion of points was higher in the DLPFC, but all individual targets in the DLPFC were within the applied FPCN mask, while in PPC some targets turned out to be beyond this mask. The analysis of the determined target localization variability allows us to state that in none of the specified areas there is a single universal position of the stimulating coil that would allow for effective stimulation of the targets in all volunteers. Moreover, according to the data obtained, the distance between the M1 zones and the DLPFC did not exceed 5 cm only in 25% of subjects, which confirmed that it was incorrect to use the routine “5 cm rule” for coil positioning, at least in the population of healthy individuals.

The personalized target selection algorithm developed allows one to determine individual localization of targets in two key FPCN hubs. The resulting target localization in volunteers was variable in both DLPFC and PPC. Moreover, the size of the stimulated area for most figure-of-eight coils most frequently used for rTMS (for the details of calculations see [22]) is smaller, than the size of the individual target dispersion area in both DLPFC and PPC. Thus, it is clear that there is no single universal stimulation coil position that would allow for effective stimulation of targets in all volunteers in any specified region. These data challenge the “one-fits-all” concept widely used in both scientific research and clinical practice, implying the use of the universal approach (the same for all subjects/patients) to determine the target in the region of interest based on the structural (for example, specified coordinates in the MNI space) or surface (for example, the “5 cm rule”) landmarks. The data showing that in the highly heterogeneous regions, such as DLPFC, the same anatomical zone can be part of different networks, so the neural network effects resulting from stimulation of this zone would be different, suggest that the concept is incorrect [23].

Comparison with the available literature data showed similarity of localization of targets in the DLPFC as a FPCN hub. Thus, the average of the targets corresponding to the peaks of the left FPCN independent component, identified visually among the independent component analysis (ICA) results, obtained in the study [24], was located at coordinates (–38, –39, 17) in the MNI space. This point is located at a distance of 7.4 mm from the midpoint obtained in our study in the direction into the depth of the brain (Fig. 4). The more superficial location of targets reported in our study is explained by methodological

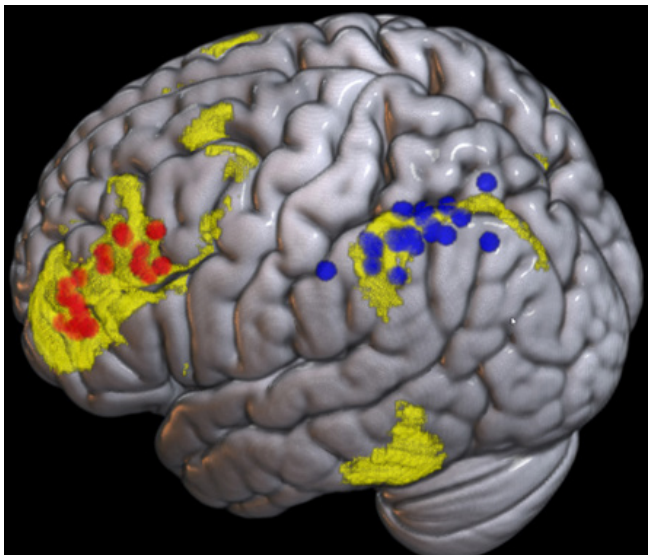

Fig. 3. Positions of targets for all subjects in the MNI space. Shown in yellow is the group-derived mask of the frontoparietal control network (FPCN) from [20] used as a seed region in the calculations of individual connectivity. Shown in red are the individual targets in DLPFC (defined as the part of the middle frontal gyrus excluding the premotor cortex), shown in blue are the targets in the posterior parietal cortex (defined as the union of the supramarginal and angular gyri and the superior parietal lobule). The data is shown on the mni152 template from the MRIcroGL software

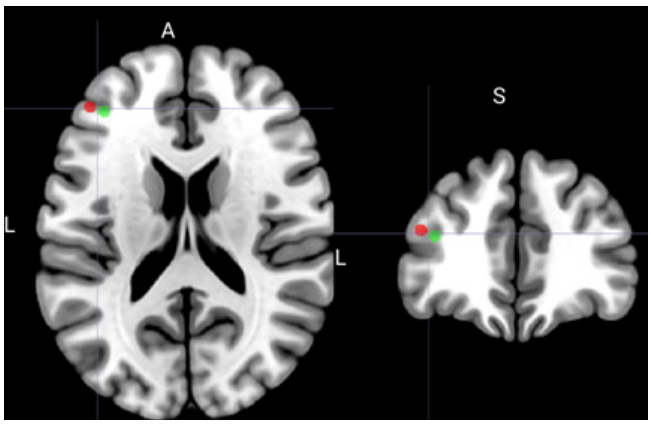

Fig. 4. Comparison of the mean target locations in the DLPFC in MNI space from this study (red) and the paper [24] (green). In the study [24], the point was calculated as the mean of targets defined as peaks of independent components of the individual resting-state fMRI signal visually identified as the FPCN.

features. Considering the limited depth of the magnetic field effect in rTMS, we limited the depth at which the targets were located by the intracranial volume margin found using the spm_erode function of the SPM package.

We have found that the mean distance between the hand zone of primary motor cortex (M1) and targets in the DLPFC exceeds 6 cm. The data obtained are important in the context of assessing the “5 cm rule” validity as an approach to localization of the rTMS target in the DLPFC. Such an approach was originally proposed in the studies focused on therapy for treatment-resistant depression [25]. However, later it became widely used for localization of targets in the DLPFC and for other disorders, as well as in the studies involving healthy volunteers due to simplicity and convenience. According to our data, the distance between the target in the DLPFC and the hand zone in M1 did not exceed 5 cm only in 25% of subjects. Furthermore, it’s important to note that we assessed the shortest distance between two points, while the “5 cm rule” implies estimation of the distance between the projections of those on the convex scalp surface. These data confirm the results of multiple studies

showing that when using the "5 cm rule" the resulting target is displaced caudally relative to the targets obtained by using neuronavigation systems based on the structural and functional data, and the target is often located within the premotor cortex, i.e. another anatomical zone having different functions and connections [26–28].

When comparing the regions formed by sets of targets in two specified regions with each other and with the FPCN mask used as a seed region, it has been shown that with comparable linear target dispersion metrics, the volume of the polyhedron, at the vertices of which the obtained individual targets lie, is significantly higher for the DLPFC than for the PPC. At the same time, all individual targets in the DLPFC are within the FPCN mask, while in the PPC some targets are beyond this mask. The findings suggest high interindividual variability of the topography of both FPCN hubs, which only emphasizes the need for the personalized approach to target selection.

The proposed algorithm for determining targets needs to be discussed separately. To find the cortical surface individual parcellation into functional resting-state network, we used an algorithm similar to the first step of the iterative method [9]: the group mask of the fronto-parietal control network from the paper [20] was used as a seed region when assessing individual resting-state fMRI data. The initial literature review showed that the MS-HBM method [11] allowing one to select the most homogeneous signal in the regions obtained seemed optimal for the task of individual determination of resting-state networks. However, this method does not allow one to assess the degree of confidence in the belonging of each point to the specified network, which is required to select the optimal point within a specified network fragment. We rejected the approaches involving the independent component analysis due to the need to match the components obtained from individual data to the known networks previously obtained using group data. Furthermore, such matching can be accomplished by both visual topography comparison [24] and automated methods [29, 30], but in both cases there can be situations with high uncertainty in the assignment of networks making it difficult to interpret the results.

The searchlight method allowing one to consider heterogeneity of the signal from neighboring voxels within the areas of interest was used to select the target based on this connectivity map. However, in this case the target localization depended on the sphere size specified by the researcher. We used a sphere radius of 5 mm, taking into account the size of the area stimulated during rTMS [22]. Thus, the algorithm developed was designed to identify individual targets for rTMS based on the FPCN hub identification.

Study limitations

The small size of the sample of subjects represents a limitation of this study. However, heterogeneity in the rTMS target location justifying the importance of a personalized approach was demonstrated even in such sample. Inclusion of healthy young and middle-aged volunteers only is another limitation, due to which in future studies it will be necessary to conduct a similar analysis in healthy older and elderly individuals, as well as in patients with cognitive impairment of different origin. It should be also noted that in this study neuroimaging was conducted in a 3 T MRI scanner. It seems reasonable to validate the proposed algorithm using data from 1–1.5 T MRI scanners, which are much more accessible. Furthermore, in this study we did not assess stability between sessions for the determined individual FPCN and the targets in the DLPFC and PPC selected based on this network. It should be noted that after the first iteration of the algorithm [9], which is conceptually similar to our method, the individual parcellation into resting-state networks for the Human Connectome Project data had a reproducibility of about 0.9, which was measured as the proportion of voxels found in the same network upon retest (though the data had approximately twice longer duration and twice higher temporal resolution).

CONCLUSIONS

Personalization of the target selection for rTMS is an important problem, the solution of which can significantly increase the effectiveness of using the method in clinical practice and scientific research. The analysis of individual resting-state network maps makes it possible to obtain personalized targets, the localization of which is characterized by high interindividual variability. At the same time it should be noted, that such analysis is associated with a number of methodological problems and requires a justified choice of one or another approach at each stage. During the study we proposed an algorithm for personalized selection of targets for rTMS based on the resting-state fMRI in the DLPFC and PPC, being the key FPCN hubs and the main rTMS targets in both patients with cognitive impairment and healthy individuals in studies of cognitive function modulation. The development of automated algorithms for the resting-state fMRI analysis accounting for the specifics of the task (determination of targets for rTMS) may further facilitate the wider spread of personalized rTMS. It is necessary to confirm the increase in rTMS effectiveness when using the developed approach to personalized target selection in further randomized controlled trials.

References

1. Chen M, Zhao G, Peng L. Transcranial Magnetic Stimulation Applications in the Study of Executive Functions: A Review. Brain Behav. 2024; 14 (11): e70099.
2. Sun W, Wu Q, Gao L, Zheng Z, Xiang H, Yang K, et al. Advancements in Transcranial Magnetic Stimulation Research and the Path to Precision. Neuropsychiatr Dis Treat. 2023; 19: 1841–51.
3. Tik M, Hoffmann A, Sladky R, Tomova L, Hummer A, Navarro de Lara L, et al. Towards understanding rTMS mechanism of action: Stimulation of the DLPFC causes network-specific increase in functional connectivity. Neuroimage. 2017; 162: 289–96.
4. Ørbo MC, Høier S, Vangberg TR, Csifcsak G, Grønli OK, Aslaksen PM. The cerebral and cognitive changes after intermittent theta burst stimulation (iTBS) treatment for depression: study protocol for a randomized double-blind sham-controlled trial. Trials. 2024; 25 (1): 752.
5. Smith S, Duff E, Groves A, Nichols TE, Jbabdi S, Westlye LT, et al. Structural Variability in the Human Brain Reflects Fine-Grained Functional Architecture at the Population Level. J Neurosci.; 39 (31): 6136–49.
6. Lioumis P, Roine T, Granö I, Aydogan DB, Ukharova E, Souza VH, et al. Optimization of TMS target engagement: current state and future perspectives. Front Neurosci. 2025; 19: 1517228.
7. Caulfield KA, Fleischmann HH, Cox CE, Wolf JP, George MS, McTeague LM. Neuronavigation maximizes accuracy and precision in TMS positioning: Evidence from 11,230 distance, angle, and electric field modeling measurements. Brain Stimul. 2022; 15 (5):

1192–205.
8. Cash RFH, Zalesky A. Personalized and Circuit-Based Transcranial Magnetic Stimulation: Evidence, Controversies, and Opportunities. Biol Psychiatry. 2024; 95 (6): 510–22.
9. Wang D, Buckner RL, Fox MD, Holt DJ, Holmes AJ, Stoecklein S, et al. Parcellating cortical functional networks in individuals. Nat Neurosci. 2015; 18 (12): 1853–60.
10. Gordon EM, Laumann TO, Gilmore AW, Newbold DJ, Greene DJ, Berg JJ, et al. Precision Functional Mapping of Individual Human Brains. Neuron. 2017; 95 (4): 791–807.e7.
11. Kong R, Li J, Orban C, Sabuncu MR, Liu H, Schaefer A, et al. Spatial Topography of Individual-Specific Cortical Networks Predicts Human Cognition, Personality, and Emotion. Cereb Cortex. 2019; 29 (6): 2533–51.
12. Ning L, Makris N, Camprodon JA, Rathi Y. Limits and reproducibility of resting-state functional MRI definition of DLPFC targets for neuromodulation. Brain Stimul. 2019; 12 (1): 129–38.
13. Fox MD, Liu H, Pascual-Leone A. Identification of reproducible individualized targets for treatment of depression with TMS based on intrinsic connectivity. Neuroimage. 2013; 66: 151–60.
14. Cash RFH, Cocchi L, Lv J, Wu Y, Fitzgerald PB, Zalesky A. Personalized connectivity-guided DLPFC-TMS for depression: Advancing computational feasibility, precision and reproducibility. Hum Brain Mapp. 2021; 42 (13): 4155–72.
15. Menon V, D'Esposito M. The role of PFC networks in cognitive control and executive function. Neuropsychopharmacology. 2022; 47 (1): 90–103.
16. Xia H, He Q, Chen A. Understanding cognitive control in aging: A brain network perspective. Front Aging Neurosci. 2022; 14: 1038756.
17. Ebrahimzadeh E, Sadjadi SM, Asgarinejad M, Dehghani A, Rajabion L, Soltanian-Zadeh H. Neuroenhancement by repetitive transcranial magnetic stimulation (rTMS) on DLPFC in healthy adults. Cogn Neurodyn. 2025; 19 (1): 34.
18. Zhang Y, Dong K, Yang J, Guo Q, Zhao Y, Zhu X, et al. Comparative efficacy of rTMS on different targets in Alzheimer's disease: a systematic review and meta-analysis. Front Aging Neurosci. 2025; 17: 1536573.
19. Xu M, Nikolin S, Samaratunga N, Chow EJH, Loo CK, Martin DM. Cognitive Effects Following Offline High-Frequency Repetitive Transcranial Magnetic Stimulation (HF-rTMS) in Healthy Populations: A Systematic Review and Meta-Analysis. Neuropsychol Rev. 2024; 34 (1): 250–76.
20. Yeo BT, Krienen FM, Sepulcre J, Sabuncu MR, Lashkari D, Hollinshead M, et al. The organization of the human cerebral cortex estimated by intrinsic functional connectivity. J Neurophysiol. 2011; 106 (3): 1125–65.
21. Hammers A, Allom R, Koepp MJ, Free SL, Myers R, et al. Three-dimensional maximum probability atlas of the human brain, with particular reference to the temporal lobe. Hum Brain Mapp. 2003;19(4):224-47.
22. Mayka MA, Corcos DM, Leurgans SE, Vaillancourt DE. Three-dimensional locations and boundaries of motor and premotor cortices as defined by functional brain imaging: a meta-analysis. Neuroimage. 2006;31(4):1453-74.
23. Van Essen DC, Smith SM, Barch DM, Behrens TE, Yacoub E, Ugurbil K; et al. The WU-Minn Human Connectome Project: an overview. Neuroimage. 2013; 80: 62–79.
24. Drakaki M, Mathiesen C, Siebner HR, Madsen K, Thielscher A. Database of 25 validated coil models for electric field simulations for TMS. Brain Stimul. 2022; 15 (3): 697–706.
25. Lynch CJ, Elbau IG, Ng TH, Wolk D, Zhu S, Ayaz A, et al. Automated optimization of TMS coil placement for personalized functional network engagement. Neuron. 2022; 110 (20): 3263–77.
26. Sayalı C, Gogulski J, Granö I, Lioumis P, Barrett F. Test-retest reliability of TMS-evoked potentials over fMRI-based definitions of non-motor cortical targets. bioRxiv 2024.12.20.629675.
27. Pascual-Leone A, Rubio B, Pallardó F, Catalá MD. Rapid-rate transcranial magnetic stimulation of left dorsolateral prefrontal cortex in drug-resistant depression. Lancet. 1996; 348 (9022): 233–7.
28. Tsukuda B, Ikeda S, Minami S, Katsura K, Shimizu T, Kame T, et al. Targeting Method for rTMS for Treating Depression in Japanese Patients: A Comparison of the Standard, F3, and Neuronavigation Approaches. Neuropsychobiology. 2024; 83 (3–4): 170–8.
29. Fitzgerald PB. Targeting repetitive transcranial magnetic stimulation in depression: do we really know what we are stimulating and how best to do it? Brain Stimul. 2021; 14 (3): 730–6.
30. Ahdab R, Ayache SS, Brugières P, Goujon C, Lefaucheur JP. Comparison of "standard" and "navigated" procedures of TMS coil positioning over motor, premotor and prefrontal targets in patients with chronic pain and depression. Neurophysiol Clin. 2010; 40 (1): 27–36.
31. Bagattini C, Brignani D, Bonnì S, Quattrini G, Gasparotti R, Pievani M. Functional Imaging to Guide Network-Based TMS Treatments: Toward a Tailored Medicine Approach in Alzheimer's Disease. Front Neurosci. 2021; 15: 687493.
32. Castrillon G, Sollmann N, Kurcyus K, Razi A, Krieg SM, Riedl V. The physiological effects of noninvasive brain stimulation fundamentally differ across the human cortex. Sci Adv. 2020; 6 (5): eaay2739.

Литература

1. Chen M, Zhao G, Peng L. Transcranial Magnetic Stimulation Applications in the Study of Executive Functions: A Review. Brain Behav. 2024; 14 (11): e70099.
2. Sun W, Wu Q, Gao L, Zheng Z, Xiang H, Yang K, et al. Advancements in Transcranial Magnetic Stimulation Research and the Path to Precision. Neuropsychiatr Dis Treat. 2023; 19: 1841–51.
3. Tik M, Hoffmann A, Sladky R, Tomova L, Hummer A, Navarro de Lara L, et al. Towards understanding rTMS mechanism of action: Stimulation of the DLPFC causes network-specific increase in functional connectivity. Neuroimage. 2017; 162: 289–96.
4. Ørbo MC, Høier S, Vangberg TR, Csifcsak G, Grønli OK, Aslaksen PM. The cerebral and cognitive changes after intermittent theta burst stimulation (iTBS) treatment for depression: study protocol for a randomized double-blind sham-controlled trial. Trials. 2024; 25 (1): 752.
5. Smith S, Duff E, Groves A, Nichols TE, Jbabdi S, Westlye LT, et al. Structural Variability in the Human Brain Reflects Fine-Grained Functional Architecture at the Population Level. J Neurosci.; 39 (31): 6136–49.
6. Lioumis P, Roine T, Granö I, Aydogan DB, Ukharova E, Souza VH, et al. Optimization of TMS target engagement: current state and future perspectives. Front Neurosci. 2025; 19: 1517228.
7. Caulfield KA, Fleischmann HH, Cox CE, Wolf JP, George MS, McTeague LM. Neuronavigation maximizes accuracy and precision in TMS positioning: Evidence from 11,230 distance, angle, and electric field modeling measurements. Brain Stimul. 2022; 15 (5): 1192–205.
8. Cash RFH, Zalesky A. Personalized and Circuit-Based Transcranial Magnetic Stimulation: Evidence, Controversies, and Opportunities. Biol Psychiatry. 2024; 95 (6): 510–22.
9. Wang D, Buckner RL, Fox MD, Holt DJ, Holmes AJ, Stoecklein S, et al. Parcellating cortical functional networks in individuals. Nat Neurosci. 2015; 18 (12): 1853–60.
10. Gordon EM, Laumann TO, Gilmore AW, Newbold DJ, Greene DJ, Berg JJ, et al. Precision Functional Mapping of Individual Human Brains. Neuron. 2017; 95 (4): 791–807.e7.
11. Kong R, Li J, Orban C, Sabuncu MR, Liu H, Schaefer A, et al. Spatial Topography of Individual-Specific Cortical Networks Predicts Human Cognition, Personality, and Emotion. Cereb Cortex. 2019; 29 (6): 2533–51.
12. Ning L, Makris N, Camprodon JA, Rathi Y. Limits and reproducibility of resting-state functional MRI definition of DLPFC targets for neuromodulation. Brain Stimul. 2019; 12 (1): 129–38.
13. Fox MD, Liu H, Pascual-Leone A. Identification of reproducible individualized targets for treatment of depression with TMS based on intrinsic connectivity. Neuroimage. 2013; 66: 151–60.
14. Cash RFH, Cocchi L, Lv J, Wu Y, Fitzgerald PB, Zalesky A. Personalized connectivity-guided DLPFC-TMS for depression:

Advancing computational feasibility, precision and reproducibility. Hum Brain Mapp. 2021; 42 (13): 4155–72.
15. Menon V, D'Esposito M. The role of PFC networks in cognitive control and executive function. Neuropsychopharmacology. 2022; 47 (1): 90–103.
16. Xia H, He Q, Chen A. Understanding cognitive control in aging: A brain network perspective. Front Aging Neurosci. 2022; 14: 1038756.
17. Ebrahimzadeh E, Sadjadi SM, Asgarinejad M, Dehghani A, Rajabion L, Soltanian-Zadeh H. Neuroenhancement by repetitive transcranial magnetic stimulation (rTMS) on DLPFC in healthy adults. Cogn Neurodyn. 2025; 19 (1): 34.
18. Zhang Y, Dong K, Yang J, Guo Q, Zhao Y, Zhu X, et al. Comparative efficacy of rTMS on different targets in Alzheimer's disease: a systematic review and meta-analysis. Front Aging Neurosci. 2025; 17: 1536573.
19. Xu M, Nikolin S, Samaratunga N, Chow EJH, Loo CK, Martin DM. Cognitive Effects Following Offline High-Frequency Repetitive Transcranial Magnetic Stimulation (HF-rTMS) in Healthy Populations: A Systematic Review and Meta-Analysis. Neuropsychol Rev. 2024; 34 (1): 250–76.
20. Yeo BT, Krienen FM, Sepulcre J, Sabuncu MR, Lashkari D, Hollinshead M, et al. The organization of the human cerebral cortex estimated by intrinsic functional connectivity. J Neurophysiol. 2011; 106 (3): 1125–65.
21. Hammers A, Allom R, Koepp MJ, Free SL, Myers R, et al. Three-dimensional maximum probability atlas of the human brain, with particular reference to the temporal lobe. Hum Brain Mapp. 2003;19(4):224-47.
22. Mayka MA, Corcos DM, Leurgans SE, Vaillancourt DE. Three-dimensional locations and boundaries of motor and premotor cortices as defined by functional brain imaging: a meta-analysis. Neuroimage. 2006;31(4):1453-74.
23. Van Essen DC, Smith SM, Barch DM, Behrens TE, Yacoub E, Ugurbil K; et al. The WU-Minn Human Connectome Project: an overview. Neuroimage. 2013; 80: 62–79.
24. Drakaki M, Mathiesen C, Siebner HR, Madsen K, Thielscher A. Database of 25 validated coil models for electric field simulations for TMS. Brain Stimul. 2022; 15 (3): 697–706.
25. Lynch CJ, Elbau IG, Ng TH, Wolk D, Zhu S, Ayaz A, et al. Automated optimization of TMS coil placement for personalized functional network engagement. Neuron. 2022; 110 (20): 3263–77.
26. Sayalı C, Gogulski J, Granö I, Lioumis P, Barrett F. Test-retest reliability of TMS-evoked potentials over fMRI-based definitions of non-motor cortical targets. bioRxiv 2024.12.20.629675.
27. Pascual-Leone A, Rubio B, Pallardó F, Catalá MD. Rapid-rate transcranial magnetic stimulation of left dorsolateral prefrontal cortex in drug-resistant depression. Lancet. 1996; 348 (9022): 233–7.
28. Tsukuda B, Ikeda S, Minami S, Katsura K, Shimizu T, Kame T, et al. Targeting Method for rTMS for Treating Depression in Japanese Patients: A Comparison of the Standard, F3, and Neuronavigation Approaches. Neuropsychobiology. 2024; 83 (3–4): 170–8.
29. Fitzgerald PB. Targeting repetitive transcranial magnetic stimulation in depression: do we really know what we are stimulating and how best to do it? Brain Stimul. 2021; 14 (3): 730–6.
30. Ahdab R, Ayache SS, Brugières P, Goujon C, Lefaucheur JP. Comparison of "standard" and "navigated" procedures of TMS coil positioning over motor, premotor and prefrontal targets in patients with chronic pain and depression. Neurophysiol Clin. 2010; 40 (1): 27–36.
31. Bagattini C, Brignani D, Bonnì S, Quattrini G, Gasparotti R, Pievani M. Functional Imaging to Guide Network-Based TMS Treatments: Toward a Tailored Medicine Approach in Alzheimer's Disease. Front Neurosci. 2021; 15: 687493.
32. Castrillon G, Sollmann N, Kurcyus K, Razi A, Krieg SM, Riedl V. The physiological effects of noninvasive brain stimulation fundamentally differ across the human cortex. Sci Adv. 2020; 6 (5): eaay2739.